

Realistic Simulations on the Continuum

12.1 Introduction and Motivations

In the previous chapters, we introduced efficient variational and projection Monte Carlo techniques, which provide very accurate descriptions of the ground-state properties of lattice models. The restriction of the electronic coordinates on a given lattice has been proven to be very useful and successful to describe many phenomena, including Anderson localization, Kondo screening, and the existence of Mott insulators. In numerical calculations, the lattice has enormous advantages because (i) configurations can be easily enumerated and most importantly (ii) there is a natural short-distance cutoff that allows us to treat the model without further approximations. Within the computational approach, the continuous limit represents a mathematical abstraction, which cannot be captured on a computer, given the finite-precision arithmetic that is at the basis of any numerical calculations. Therefore, we can imagine that the continuous space is obtained by considering a lattice with spacing a and taking the limit $a \rightarrow 0$. In this case, electrons hop performing discrete jumps of length a and interact through the original Coulomb potential. This approach is called “lattice regularization” and provides the advantage that, for any given lattice spacing a , the system can be directly simulated in the computer. Then, we are able to get the correct physical properties of the continuous Hamiltonian by taking sufficiently small lattice spacings.

However, within the variational approach, whenever the wave function is expressed in terms of few parameters (McMillan, 1965; Ceperley et al., 1977), the lattice regularization introduces an unnecessary approximation, without improving the efficiency of the algorithm. Nevertheless, we can be tempted to use the lattice regularization to consider a systematic parametrization of the wave function on a grid. Unfortunately, this kind of approach is not suitable for *ab-initio* calculations of realistic materials, whenever a full optimization of the electronic orbitals is

desirable; indeed, the lattice regularization would introduce too many parameters that cannot be handled at present within stochastic techniques. For example, let us consider liquid Hydrogen with 200 atoms (corresponding to the same number of electrons and 100 molecular orbitals) in a $100 \times 100 \times 100$ grid; this case would imply 10^8 variational parameters, which is impossible to handle by any stochastic optimization method: despite the remarkable progress in recent years, at present this number cannot exceed $\approx 10^4$ (Neuscamman et al., 2012). Therefore, as in lattice models, the variational state can be written as a product of an uncorrelated (e.g., Slater) part, which embodies the correct anti-symmetric fermionic properties, and a correlation (e.g., Jastrow) factor, which includes correlation among electrons. The Slater part of the wave function is usually obtained by using a deterministic mean-field approach, where the problem of having many variational parameters can be tackled by using very cheap and efficient self-consistent methods. Then, the Slater part is not changed in presence of the Jastrow factor, which can be optimized by using a suitable parametrization (Filippi and Umrigar, 1996; Wagner et al., 2009; Needs et al., 2010; Kim et al., 2012).

Here, we want to follow the idea that the Slater determinant given by a mean-field-like approach is not the optimal solution. Indeed, whenever the mean field does not describe correctly the system, this procedure has no hope to capture the correct low-energy behavior. For example, within this kind of approach, we will never be able to describe superconductivity driven by repulsive interactions only. Instead, a qualitative correct description of the ground state can be achieved by including a correlation (e.g., Jastrow) factor, even when the Slater determinant is built from a small basis set but it is optimized in presence of the Jastrow factor. In this case, the optimization procedure can be mapped into an iterative linear problem in a reduced sub-space spanned by the variational parameters. We remark that an optimized wave function with a limited number of parameters corresponds to the ground state of a local Hamiltonian that, for a good *Ansatz*, is “sufficiently close” to the original one. By contrast, a variational approach may be intrinsically biased because it cannot describe properties that have not been explicitly considered in the wave function. Nevertheless, in our opinion, the variational method is tremendously important, even in presence of this limitation, since a black-box tool that solves the electron problem does not exist yet. Indeed, for a given system, we should be able to construct reasonable wave functions and get quantitative results. Then, this method can be validated by explicit and direct comparison with experiments, without tunable parameters, because the variational wave function is determined unambiguously (i.e., by an *ab-initio* procedure) by the minimization of the expectation value of the energy. Moreover, the variational approach will remain useful even when it does not compare favorably with experiments, since this case will falsify the form of the wave function, stimulating the introduction

of new physical ingredients in it. In this spirit, we mention successful examples, as the resonating valence-bond state introduced by Anderson (1987) to describe High-temperature superconductivity and the Laughlin (1983) wave function for the fractional quantum Hall effect.

12.2 Variational Wave Function with Localized Orbitals

Here, we discuss the general form of the correlated wave functions that we use for the continuum case. We denote the coordinates of the N_e electrons with $\mathbf{x} = \{\mathbf{r}_1, \dots, \mathbf{r}_{N_e}\}$. In the following, we will consider an equal number of spin-up and spin-down electrons (i.e., $N_e/2$ pairs of electrons with opposite spins). For practical purposes, we can fix the spin of each electron in such a way that the first (last) $N_e/2$ particles have spin-up (spin-down). Within this choice, the coordinates of the spin-up and spin-down electrons are denoted by $\{\mathbf{r}_i^\uparrow\}$ and $\{\mathbf{r}_i^\downarrow\}$ (with $i = 1, \dots, N_e/2$), respectively. Then, because of the Pauli principle, the orbital part of the variational wave function $\Psi(\mathbf{x})$ (associated to this spin configuration) must be anti-symmetric for all exchanges of particles with the same spin (while there are no symmetry properties when exchanging particles with opposite spins). The variational *Ansatz* for the many-body state is written as the product of two terms:

$$\Psi(\mathbf{x}) = \mathcal{J}(\mathbf{x})F(\mathbf{x}), \quad (12.1)$$

where the (positive) Jastrow factor $\mathcal{J}(\mathbf{x})$ is symmetric under all the permutations among the coordinates of the particles and is given in terms of the two-body pseudo-potential $u(\mathbf{r}, \mathbf{r}')$:

$$\mathcal{J}(\mathbf{x}) = \exp \left[\sum_{i < j} u(\mathbf{r}_i, \mathbf{r}_j) \right], \quad (12.2)$$

and the determinant part $F(\mathbf{x})$, enforcing the anti-symmetry among the particles with the same spin, is defined in terms of the pairing function $f(\mathbf{r}, \mathbf{r}')$ (defined in the configuration space):

$$F(\mathbf{x}) = \det f \left(\mathbf{r}_i^\uparrow, \mathbf{r}_j^\downarrow \right). \quad (12.3)$$

In the following, we will restrict ourselves to the case of a *singlet* wave function, implying that the pairing function is symmetric, i.e., $f(\mathbf{r}, \mathbf{r}') = f(\mathbf{r}', \mathbf{r})$ (which, in most cases, is also taken *real*).

The determinant, which is computed in terms of the $N_e/2 \times N_e/2$ matrix of the pairing function is called *anti-symmetrized geminal power* (AGP). We remark that the uncorrelated part $F(\mathbf{x})$ can be reduced to a Slater determinant for particular choices of the pairing function (see below), but it allows us to obtain much

more general quantum states, like for example BCS superconductors. Moreover, it is important to emphasize that, similarly to what happens in lattice models, the Jastrow factor is the simplest term to describe the Coulomb repulsion between electrons, introducing a “renormalization” of the uncorrelated $F(\mathbf{x})$ when two electrons are very close. This effect cannot be taken into account by any one-electron *Ansatz*, since, in such a case, each electron behaves as an independent particle that experiences a mean-field potential determined by the average effect of all the other electrons. By using the above expression, a standard variational Monte Carlo approach is possible, allowing the evaluation of the expectation value of the energy and correlation functions, with a computational time that scales with $O(N_e^3)$ (Ceperley et al., 1977).

Here, we describe in detail how the two functions $u(\mathbf{r}, \mathbf{r})$ and $f(\mathbf{r}, \mathbf{r}')$ (entering in the definition of the Jastrow factor and the determinant part, respectively) can be conveniently expanded by using a set of *atomic orbitals*. For this purpose, we consider an atomic basis $\{\phi_p(\mathbf{r} - \mathbf{R}_I)\}$, where each element has an orbital index p and depends upon a given index I , denoting the ion where the orbital is centered. Here, $p = 1, \dots, N_{\text{orb}}(I)$ and $I = 1, \dots, N_{\text{ion}}$, $N_{\text{orb}}(I)$ and N_{ion} being the total number of orbitals associated to a given ion I and the number of ions, respectively. In the following, to simplify the notation, we use a single index μ to indicate both the orbital p and the atomic center I , leading to $\{\phi_\mu(\mathbf{r})\}$. Within this compact notation, both the positions of the ions and the orbital indices are integer functions of μ , namely $I = I(\mu)$ and $p = p(\mu)$.

The atomic basis is not necessarily orthonormal. Actually, for practical purposes, it is convenient to choose simple (e.g., Slater or Gaussian, see below) localized orbitals. In this scheme, we define the overlap matrix \mathbf{S} by:

$$S_{\mu,v} = \int d\mathbf{r} \phi_\mu(\mathbf{r})\phi_v(\mathbf{r}). \quad (12.4)$$

In practice, the matrix \mathbf{S} can be computed exactly for Gaussian orbitals in open systems; nevertheless, we have experienced that a very good approximation can be also obtained by using a finite mesh of lattice points and then evaluating numerically the corresponding integrals. This latter approach is very general and allows us to consider also Slater orbitals (and even more general ones). We also emphasize that, on modern supercomputers, the numerical evaluation of \mathbf{S} is very efficient and usually requires a negligible computational effort.

Then, the pairing function can be generally written as:

$$f(\mathbf{r}, \mathbf{r}') = \sum_{\mu,v} f_{\mu,v} \phi_\mu(\mathbf{r})\phi_v(\mathbf{r}'), \quad (12.5)$$

where $f_{\mu,\nu}$ defines a real and symmetric matrix. We point out that, whenever the atomic basis is large enough, it is possible to represent any (normalizable) function $f(\mathbf{r}, \mathbf{r}')$ exactly. Analogously, the correlation term $u(\mathbf{r}_i, \mathbf{r}_j)$ can be also expanded in a possibly distinct set of atomic orbitals $\{\chi_\mu(\mathbf{r})\}$, with the same compact notation used before. However, in order to speed up the convergence to the complete basis set limit (or, in other words, to parametrize satisfactorily the Jastrow term within a small basis), it is important to fulfill the so-called cusp conditions that are implied by the divergence of the Coulomb potential at short distances. In this way, the leading singular behaviors when $\mathbf{r} \rightarrow \mathbf{r}'$ (electron-electron) or when $\mathbf{r} \rightarrow \mathbf{R}_I$ (electron-ion) are satisfied exactly, namely $u(\mathbf{r}, \mathbf{r}') \approx |\mathbf{r} - \mathbf{r}'|/2$ and $u(\mathbf{r}, \mathbf{r}') \approx -Z_I|\mathbf{r} - \mathbf{R}_I|/(N_e - 1)$ (where Z_I indicates the charge number of the atom I), respectively. Therefore, the general form of the correlator factor $u(\mathbf{r}, \mathbf{r}')$ is written as (here, we assume that $N_e > 1$):

$$u(\mathbf{r}, \mathbf{r}') = \left[\frac{u_{\text{ei}}(\mathbf{r}) + u_{\text{ei}}(\mathbf{r}')}{N_e - 1} \right] + u_{\text{ee}}(\mathbf{r}, \mathbf{r}'), \quad (12.6)$$

where the first two terms in the bracket describe the electron-ion interaction and the third one is related to the genuine electron-electron correlations:

$$u_{\text{ei}}(\mathbf{r}) = u_{\text{ei}}^{\text{cusp}}(\mathbf{r}) + \sum_{\nu} w_{\nu} \chi_{\nu}(\mathbf{r}), \quad (12.7)$$

$$u_{\text{ee}}(\mathbf{r}, \mathbf{r}') = u_{\text{ee}}^{\text{cusp}}(\mathbf{r}, \mathbf{r}') + \sum_{\mu,\nu} u_{\mu,\nu} \chi_{\mu}(\mathbf{r}) \chi_{\nu}(\mathbf{r}'); \quad (12.8)$$

here, $u_{\text{ei}}^{\text{cusp}}(\mathbf{r})$ and $u_{\text{ee}}^{\text{cusp}}(\mathbf{r}, \mathbf{r}')$ are assumed to satisfy the electron-electron and electron-ion cusp conditions, respectively. The simplest expressions that are always bounded and widely used are (Foulkes et al., 2001):

$$u_{\text{ei}}^{\text{cusp}}(\mathbf{r}) = - \sum_I \frac{Z_I |\mathbf{r} - \mathbf{R}_I|}{1 + \sqrt{2Z_I} b_{\text{ei}} |\mathbf{r} - \mathbf{R}_I|}, \quad (12.9)$$

$$u_{\text{ee}}^{\text{cusp}}(\mathbf{r}, \mathbf{r}') = \frac{|\mathbf{r} - \mathbf{r}'|}{2(1 + b_{\text{ee}} |\mathbf{r} - \mathbf{r}'|)}, \quad (12.10)$$

where b_{ei} and b_{ee} are two independent (positive) variational parameters. In addition, $u_{\mu,\nu}$ is a symmetric matrix and w_{ν} is a vector, which describe the variational freedom of the Jastrow factor in the given (finite) atomic basis. The reason to scale the one-body contribution by $1/(N_e - 1)$ follows from the identity:

$$\exp \left\{ \sum_{i < j} \left[\frac{u_{\text{ei}}(\mathbf{r}_i) + u_{\text{ei}}(\mathbf{r}'_j)}{N_e - 1} \right] \right\} = \exp \left[\sum_i u_{\text{ei}}(\mathbf{r}_i) \right], \quad (12.11)$$

as the r.h.s. of the above equation is the commonly adopted expression for a one-body Jastrow factor in Eq. (12.2). Notice that a general and complete description of both the one-body and two-body terms can be achieved taking a sufficiently large basis set and using appropriate values for $u_{\mu,v}$ and w_v .

In practice, we can adopt the same basis set for both the Jastrow factor and the pairing function. However, usually the dimension of the basis set for the Jastrow term (D_u , including both electron-ion and electron-electron terms) can be taken much smaller than the one used for the pairing function (D_f), since converged results for various chemical properties can be achieved with a small value of D_u . In summary, we are led to optimize a total number of parameters:

$$N_{\text{par}} = \frac{D_f(D_f + 1) + D_u(D_u + 1)}{2} + D_u. \quad (12.12)$$

Fortunately, similarly to what happens in quantum chemistry calculations, a very small basis is enough to describe rather accurately an electronic wave function, even in the presence of electron correlations. Indeed, the largest energy scale of the problem is the strong electron-ion attraction, which represents the main contribution for large values of Z_I and can be very accurately represented with an appropriate atomic basis containing only few elements.

12.2.1 Atomic Orbitals

Here, we would like to discuss the form of the atomic orbitals $\{\phi_{\mu}(\mathbf{r})\}$, centered at the position \mathbf{R}_I and written in terms of the radial vector $\mathbf{r} - \mathbf{R}_I$ that connects the position \mathbf{r} of the electron to the position \mathbf{R}_I of the ion I . Notice that, in the most general case, there are several orbitals that are defined on a given atom I (which defines the atomic basis on the ion I). The *elementary* objects are determined by a radial part, which is given by a Gaussian or a Slater form, and an angular part, characterized by an angular momentum l and its projection m along the z axis. On the one hand, the Gaussian form is given by:

$$\phi_{l,\pm|m|,I}^G(\mathbf{r}; \zeta) \propto |\mathbf{r} - \mathbf{R}_I|^l e^{-\zeta|\mathbf{r} - \mathbf{R}_I|^2} [Y_{l,m,I}(\boldsymbol{\Omega}) \pm Y_{l,-m,I}(\boldsymbol{\Omega})]; \quad (12.13)$$

on the other hand, the Slater form is:

$$\phi_{l,\pm|m|,I}^S(\mathbf{r}; \zeta) \propto |\mathbf{r} - \mathbf{R}_I|^l e^{-\zeta|\mathbf{r} - \mathbf{R}_I|} [Y_{l,m,I}(\boldsymbol{\Omega}) \pm Y_{l,-m,I}(\boldsymbol{\Omega})]; \quad (12.14)$$

in both cases, $Y_{l,m,I}(\boldsymbol{\Omega})$ indicates a spherical harmonic centered around \mathbf{R}_I (that depends upon the unit vector $\boldsymbol{\Omega}$); for each value of the angular momentum l (and its projection along the z axis m), the Slater and Gaussian orbitals depend upon the (variational) parameter ζ . By considering the linear combination of $Y_{l,m,I}(\boldsymbol{\Omega})$ with its complex conjugate $Y_{l,-m,I}(\boldsymbol{\Omega})$ (for $m \neq 0$), we get a real atomic basis

set; the $m = 0$ case does not require any symmetrization, being $Y_{l,0,l}$ already real. These orbitals can have a simple cartesian representation, which can be efficiently implemented.

The most general atomic orbital $\phi_\mu^{\text{contr}}(\mathbf{r})$ can be written as a linear combination of Gaussian or Slater orbitals (denoted by $X = G$ or S), everyone associated to an angular momentum l and specified by an additional index k . Then, the variational parameter ζ may acquire a dependence on l and k ; the contracted orbital is finally given by:

$$\phi_\mu^{\text{contr}}(\mathbf{r}) = \sum_{k,l,m} c_{l,m,l}^k \phi_{l,m,l}^{X_{k,l}}(\mathbf{r}, \zeta_{k,l}). \quad (12.15)$$

In quantum chemistry, this kind of linear combination is called *contraction* and is adopted to reduce the dimension of the atomic basis to describe strongly-localized atomic orbitals (e.g., $1s$), even though it is not very common to hybridize states with different angular momenta. However, in quantum chemistry, the reduction of the atomic basis set is not crucial and the main computational advantage is achieved by using a small number of molecular orbitals. By contrast, in quantum Monte Carlo approaches, it is extremely important to minimize the number of variational parameters and, therefore, it is necessary to reduce the atomic basis dimension D_f as much as possible. Then, it is recommended to reduce D_f by optimizing a number of independent atomic orbitals of the form given in Eq. (12.15), in a large basis of elementary functions. In this way, a small number of contracted orbitals is necessary to reach converged or, at least, accurate results. Thus, this kind of orbitals are generalized hybrid orbitals and appear to be of fundamental importance for describing wave functions in a compact and efficient way (Sorella et al., 2015).

As commonly done in standard electronic structure approaches (Dovesi et al., 2014), both Gaussian and Slater orbitals can be generalized to periodic systems by considering a $L_x \times L_y \times L_z$ supercell. This can be conveniently done by means of vectors $\mathbf{L}_{n_x, n_y, n_z} = (n_x L_x, n_y L_y, n_z L_z)$, labeling all possible periodic images, and by evaluating the sum for generic twisted-boundary conditions (determined by the angles $|\theta_x|$, $|\theta_y|$, and $|\theta_z| \leq \pi$):

$$\phi_{l,m,l}^{G_{\text{PBC}}, S_{\text{PBC}}}(\mathbf{r}; \zeta) = \sum_{n_x, n_y, n_z} \phi_{l,m,l}^{G,S}(\mathbf{r} + \mathbf{L}_{n_x, n_y, n_z}; \zeta) e^{i(n_x \theta_x + n_y \theta_y + n_z \theta_z)}. \quad (12.16)$$

The presence of the Gaussian or exponential factors guarantees that the above series rapidly converges. This new basis satisfies twisted-boundary conditions:

$$\phi_{l,m,l}^{G_{\text{PBC}}, S_{\text{PBC}}}(\mathbf{r} + \mathbf{L}_{n_x, n_y, n_z}; \zeta) = e^{-i(n_x \theta_x + n_y \theta_y + n_z \theta_z)} \phi_{l,m,l}^{G_{\text{PBC}}, S_{\text{PBC}}}(\mathbf{r}; \zeta), \quad (12.17)$$

which are important to study bulk properties of materials. For example, by using suitably chosen values of the twist (Baldereschi, 1973) or averaging the physical

observables over all possible angles (Lin et al., 2001), it is possible to have a smooth and rapid convergence to the thermodynamic limit.

The same procedure can be applied to the orbitals of the Jastrow factor, with $\phi_{l,\pm|m|,I}^{S,G}(\mathbf{r}; \zeta) \rightarrow \chi_{l,\pm|m|,I}^{S,G}(\mathbf{r}; \zeta)$. However, since the Jastrow factor only couples local densities, we limit ourselves to a periodic case with $\theta_x = \theta_y = \theta_z = 0$, which implies $\chi_{l,m,I}^{GPBC,SPBC}(\mathbf{r} + \mathbf{L}_{n_x, n_y, n_z}; \zeta) = \chi_{l,m,I}^{GPBC,SPBC}(\mathbf{r}; \zeta)$. Finally, the one- and two-body functions $u_{ei}^{\text{cusp}}(\mathbf{r})$ and $u_{ee}^{\text{cusp}}(\mathbf{r}, \mathbf{r}')$, defined in Eqs. (12.9) and (12.10), are slowly decaying functions and, therefore, it is convenient to express them in terms of a periodic generalization of the Euclidean distance:

$$|\mathbf{r}| \rightarrow \sqrt{\left[\frac{L_x}{\pi} \sin\left(\frac{\pi x}{L_x}\right) \right]^2 + \left[\frac{L_y}{\pi} \sin\left(\frac{\pi y}{L_y}\right) \right]^2 + \left[\frac{L_z}{\pi} \sin\left(\frac{\pi z}{L_z}\right) \right]^2}. \quad (12.18)$$

12.2.2 Molecular Orbitals

Now, we consider a different functional form for representing the uncorrelated state described by the pairing function $f(\mathbf{r}, \mathbf{r}')$. In this way, the relation between the AGP wave function and the Slater determinant will be very transparent. The (real and symmetric) pairing function can be considered as a linear operator in the continuum space; therefore, it can be diagonalized, by looking for eigenfunctions $\Phi_\alpha(\mathbf{r})$ that satisfy:

$$\int d\mathbf{r}' f(\mathbf{r}, \mathbf{r}') \Phi_\alpha(\mathbf{r}') = \lambda_\alpha \Phi_\alpha(\mathbf{r}), \quad (12.19)$$

where λ_α are the corresponding eigenvalues. In the finite basis $\{\phi_\mu(\mathbf{r})\}$ of dimension D_f , the eigenfunctions can be written as:

$$\Phi_\alpha(\mathbf{r}) = \sum_{\mu} P_{\mu,\alpha} \phi_\mu(\mathbf{r}). \quad (12.20)$$

where the elements of the matrix \mathbf{P} are found from the generalized eigenvalue equation that is obtained by substituting this expression, as well as the expansion of the pairing function (12.5), in Eq. (12.19). In this way, we obtain that:

$$\mathbf{fSP} = \mathbf{PA}, \quad (12.21)$$

where \mathbf{A} is the diagonal matrix containing the eigenvalues λ_α , \mathbf{S} is the overlap matrix of Eq. (12.4), and \mathbf{f} is the matrix with elements $f_{\mu,\nu}$ of Eq. (12.5). Notice that, as the result of the generalized eigenvalue problem, the matrix \mathbf{P} defines a set of orthonormal states:

$$\int d\mathbf{r} \Phi_\alpha(\mathbf{r}) \Phi_\beta(\mathbf{r}) = \delta_{\alpha,\beta}, \quad (12.22)$$

which leads to $\mathbf{P}^T \mathbf{S} \mathbf{P} = \mathbf{1}$. The one-body wave functions $\{\Phi_\alpha(\mathbf{r})\}$ are generally called *molecular orbitals*. Notice that, depending on the properties of the matrix \mathbf{P} , the molecular orbitals may be either *localized* or *extended*.

Finally, from Eq. (12.19), the pairing function can be written in terms of the molecular orbitals:

$$f(\mathbf{r}, \mathbf{r}') = \sum_{\alpha=1}^{D_f} \lambda_\alpha \Phi_\alpha(\mathbf{r}) \Phi_\alpha(\mathbf{r}'). \quad (12.23)$$

Remarkably, whenever the number of non-zero eigenvalues λ_α is equal to the number of electron pairs $N_e/2$, the determinant $F(\mathbf{x})$ in Eq. (12.3) can be written as the product of three square matrices of dimension $N_e/2 \times N_e/2$:

$$\det f(\mathbf{r}_i^\uparrow, \mathbf{r}_j^\downarrow) = \det(\mathbf{P}_\uparrow \tilde{\mathbf{\Lambda}} \mathbf{P}_\downarrow^T) = \left(\prod_{\alpha=1}^{N_e/2} \lambda_\alpha \right) \times \det \mathbf{P}_\uparrow \times \det \mathbf{P}_\downarrow \quad (12.24)$$

where $\tilde{\mathbf{\Lambda}}$ is the square (diagonal) matrix containing the non-zero eigenvalues only; the matrices \mathbf{P}_\uparrow and \mathbf{P}_\downarrow are given by:

$$(P_\uparrow)_{i,\alpha} = \Phi_\alpha(\mathbf{r}_i^\uparrow), \quad (12.25)$$

$$(P_\downarrow)_{i,\alpha} = \Phi_\alpha(\mathbf{r}_i^\downarrow). \quad (12.26)$$

Therefore, in this special case, we obtain a form that is consistent with the standard expression of a Slater determinant (apart from the irrelevant constant, i.e., the product of non-zero eigenvalues), i.e., the AGP wave function reduces to a Slater determinant with $N_e/2$ molecular orbitals. In other words, the molecular orbitals, which have been defined within the AGP formalism, coincide with the ones that are widely used to define Slater determinants.

The representation of a simple determinant as an AGP state, with a constrained number of molecular orbitals, has important advantages from the numerical point of view. The simplest one is to consider only one determinant of a $N_e/2 \times N_e/2$ matrix to evaluate the wave function by means of Eq. (12.3); by contrast, within the standard representation of the Slater determinant, we would need two determinants of the same dimension. Another advantage comes from the fact that it is possible to exploit symmetries, such as the translation invariance in a crystal, in a simple way. In this case, it is enough to require that the pairing matrix \mathbf{f} , corresponding to the same type of orbitals, depends only on the difference between the ion positions, i.e., $f_{\mu,v} = f_{\mu',v'}$ if $|\mathbf{R}_{I(\mu')} - \mathbf{R}_{I(v')}| = |\mathbf{R}_{I(\mu)} - \mathbf{R}_{I(v)}|$, which represents a very simple linear constraint.

Finally, we also remark that, even when the AGP state is exactly equivalent to a Slater determinant, the combined optimization of the Jastrow factor and the molecular orbitals may lead to a qualitatively different wave function, namely

with chemical and physical properties that are different from the ones obtained within uncorrelated Hartree-Fock or density-functional theory. The fully optimized Jastrow-Slater wave function with $N_e/2$ molecular orbitals provides an accurate description of atoms (Foulkes et al., 2001), with about 90% of the correlation energy (defined as the energy difference between the estimated exact result, obtained by experiments or high-quality calculations, and the best Hartree-Fock value). By releasing the constraint on the molecular orbitals, we reach a larger variational freedom; it is then obvious that the unconstrained AGP wave function can improve the Hartree-Fock approach, especially when also the Jastrow factor is included, leading to an improvement of the accuracy of the chemical bond or even to new qualitative properties. In particular, the AGP state, allowing an explicit pairing between electrons, can describe superconductors and, in presence of a Jastrow factor, also Mott (resonating-valence bond) insulators, as introduced by Anderson (1987) soon after the discovery of high-temperature superconductors.

12.3 Size Consistency of the Variational Wave Functions

A basic notion in quantum chemistry is the so-called size consistency, stating that, whenever we compute the energy of a molecular system in which we clearly distinguish two regions A and B that are spatially well separated, the total energy of the composed system E_{A+B} should be equal to the sum of the energies of the isolated systems E_A and E_B , i.e., $E_{A+B} = E_A + E_B$. The size consistency crucially affects the chemical bond and, therefore, it is considered as one of the most important properties of a wave function that is consistently optimized within its full variational freedom. It is well known that, in general, the AGP wave function is not size consistent, even when the simple Hartree-Fock state is not affected by this problem. Therefore, AGP states have been abandoned in chemistry. Within the AGP approach, size inconsistency originates from projecting over a given number of particles. For example, let us consider the Be_2 molecule, where the two regions A and B contain a single Be atom; then, the AGP wave function for the single atom implies correctly only two electron pairs. However, in the molecule, the constraint on the number of electrons would act only on the total number of four pairs. Thus, the AGP wave function for the $A + B$ system would also allow the case in which there are three or even four pairs close to a given atom and one or zero pairs close to the other one. When the molecule is stretched and the two atoms are at very large distances, this effect will not produce two independent atomic AGP wave functions, as projecting the total number of electrons is not equivalent to projecting the number of electrons in each atom. Therefore, the corresponding energy will be much higher than the one of two independent Be atoms and size consistency will be not verified.

Here, we show that, whenever the AGP wave function is combined with the Jastrow factor, the size consistency is recovered, since the latter one has the variational freedom to allow partial number projections on different space regions (Sorella et al., 2007; Neuscamman, 2012). For this purpose, we can consider a Jastrow factor that projects out all the electronic configurations that do not have exactly N_A and N_B particles in the region A and B , respectively:

$$\mathcal{J}(\mathbf{x}) \propto \exp \left\{ -\frac{C}{2} [N_A(\mathbf{x}) - N_A]^2 + A \rightarrow B \right\}, \quad (12.27)$$

where $N_{A,B}(\mathbf{x}) = \sum_i g_{A,B}(\mathbf{r}_i)$, with $g_A(\mathbf{r}) = 1$ [$g_B(\mathbf{r}) = 1$] if $\mathbf{r} \in A$ ($\mathbf{r} \in B$) and zero otherwise, and C is a sufficiently large constant. This form of the Jastrow factor can be obtained by taking a particular form of the pseudo-potential given by:

$$u(\mathbf{r}, \mathbf{r}') = -C \left\{ g_A(\mathbf{r})g_A(\mathbf{r}') - \frac{N_A - 1/2}{N_e - 1} [g_A(\mathbf{r}) + g_A(\mathbf{r}')] + A \rightarrow B \right\}. \quad (12.28)$$

Therefore, whenever the basis set of the Jastrow factor is large enough to represent the form given by Eq. (12.28), a full optimization of the global wave function guarantees that the total energy will be below the one of the two fragments (when the two regions A and B are well separated), thus implying size consistency. A *caveat* of the previous rule applies to the case in which the two fragments have non-zero spin: in this case, a wave function that is built from a single determinant is often not size consistent (e.g., the case of two Oxygen atoms, for which each independent atom has $S = 1$, while the O_2 molecule has $S = 0$). In this respect, the restricted Hartree-Fock determinant is not size consistent whenever the whole system has not the maximum spin compatible with the two fragments.

12.4 Optimization of the Variational Wave Functions

A straightforward way to optimize the pairing function is to consider all the matrix elements $f_{\mu,v}$ in Eq. (12.5) as independent variational parameters. This would be an *unconstrained* optimization. However, this way of proceeding is not always efficient, since the variational energy may have a very weak dependence on long-range pairings, especially for insulating phases. The main advantage of having a pairing function that is explicitly defined in terms of a localized basis set is the possibility to exploit the locality of the correlations. Whenever the geminal function $f(\mathbf{r}, \mathbf{r}')$ is described by a characteristic length ξ , a useful way to reduce the number of variational parameters is to consider in the optimization only matrix elements $f_{\mu,v}$ connecting orbitals at a distance smaller than a certain cutoff R_{cut} . For a given R_{cut} , for each column (or row) of the matrix $f_{\mu,v}$, only a fixed number of elements will be non-zero and, therefore, the total number of parameters scales as the total

atomic basis dimension, leading to a number of variational parameters $N_{\text{par}} \propto D_f \propto N_e$. This approach is much more efficient than an unconstrained minimization where all the matrix elements $f_{\mu,\nu}$ are independently optimized. Whenever a finite correlation length is present in the physical problem, the accuracy should improve exponentially by increasing R_{cut} . For example, if the rank of the geminal matrix is equal to half the number of electrons $N_e/2$, the geminal function corresponds to the density matrix $\rho(\mathbf{r}, \mathbf{r}')$. Then, within insulating phases, we have that:

$$\lim_{|\mathbf{r}-\mathbf{r}'| \rightarrow \infty} \rho(\mathbf{r}, \mathbf{r}') \propto \exp\left(-\frac{|\mathbf{r}-\mathbf{r}'|}{\xi}\right), \quad (12.29)$$

which justifies the inclusion of R_{cut} for an efficient minimization of the number of parameters. Unfortunately, this approach becomes quite inefficient when considering metallic phases, where (in three spatial dimensions):

$$\lim_{|\mathbf{r}-\mathbf{r}'| \rightarrow \infty} |\rho(\mathbf{r}, \mathbf{r}')| \propto \frac{1}{|\mathbf{r}-\mathbf{r}'|^2}, \quad (12.30)$$

which implies a very slow convergence with R_{cut} . The reason for this slow decay of the density matrix is due to the existence of a Fermi surface that constrains the occupation within partially filled bands.

Here, we define a *constrained* optimization procedure that is able to deal with both insulating and metallic behaviors, even in presence of a finite cutoff R_{cut} . This result can be achieved by fixing the rank of the pairing function to a given number n , namely by taking only n molecular orbitals in the definition of the geminal function:

$$f^c(\mathbf{r}, \mathbf{r}') = \sum_{\alpha=1}^n \lambda_{\alpha} \Phi_{\alpha}(\mathbf{r}) \Phi_{\alpha}(\mathbf{r}'), \quad (12.31)$$

where the molecular orbitals $\{\Phi_{\alpha}(\mathbf{r})\}$ with $\alpha = 1, \dots, n$ define the “occupied” states. Within this procedure, a Fermi surface can be “reconstructed” by imposing the mentioned constraint of n occupied states, thus allowing us to recover slowly decaying density matrices. We have three main advantages by constraining the optimization of the pairing function with a form given by a finite number n of molecular orbitals. The first one is the dual representation of the pairing function, which allows us to consider the matrix elements $f_{\mu,\nu}$ as variational parameters with the constraint of a fixed rank n or equivalently a fixed number n of optimized molecular orbitals; the second one is that, within an optimization procedure, we can initialize the pairing function (i.e., the matrix $f_{\mu,\nu}$) by taking the molecular orbitals $\Phi_{\alpha}(\mathbf{r})$ from a mean-field method defined in the same localized basis, such as Hartree-Fock or density-functional theory; the third one is that we can implement locality within a constrained approach, highly reducing the number of variational

parameters, without affecting much the accuracy of the calculation, since the long-range part of the pairing function is automatically taken into account by constraining the number of molecular orbitals, namely by forcing the presence of the Fermi surface.

Before discussing the technical details, we would like to mention that on a lattice we have used a different approach to minimize the variational parameters (see Chapters 5 and 6). There, we considered a parametrization given by an effective (BCS) Hamiltonian with finite range (i.e., parameters corresponding only to distances smaller than R_{cut}); the ground state of this effective Hamiltonian implicitly defined the pairing function, which was long range in the case of a metal or a gapless superconductor. In continuous systems, it is difficult to implement an approach that is based upon an auxiliary Hamiltonian and it is much easier to work directly with the pairing function.

For a constrained pairing function with a fixed rank n , by performing an infinitesimal change and keeping the same rank, we obtain that:

$$\delta f^c(\mathbf{r}, \mathbf{r}') = \sum_{\alpha=1}^n \delta \lambda_{\alpha} \Phi_{\alpha}(\mathbf{r}) \Phi_{\alpha}(\mathbf{r}') + \lambda_{\alpha} [\delta \Phi_{\alpha}(\mathbf{r}) \Phi_{\alpha}(\mathbf{r}') + \Phi_{\alpha}(\mathbf{r}) \delta \Phi_{\alpha}(\mathbf{r}')]. \quad (12.32)$$

Then, we can easily verify that this kind of modification satisfies the following condition (which is obtained by using the orthonormalization of the original molecular orbitals):

$$\int d\mathbf{r}_1 \int d\mathbf{r}_2 [\delta(\mathbf{r} - \mathbf{r}_1) - \Pi(\mathbf{r}, \mathbf{r}_1)] \delta f^c(\mathbf{r}_1, \mathbf{r}_2) [\delta(\mathbf{r}' - \mathbf{r}_2) - \Pi(\mathbf{r}_2, \mathbf{r}')] = 0, \quad (12.33)$$

where the projector onto the occupied states $\Pi(\mathbf{r}, \mathbf{r}')$ is given by:

$$\Pi(\mathbf{r}, \mathbf{r}') = \sum_{\alpha=1}^n \Phi_{\alpha}(\mathbf{r}) \Phi_{\alpha}(\mathbf{r}'). \quad (12.34)$$

In matrix notations, corresponding to the finite basis *Ansatz* in Eq. (12.5), Eq. (12.33) becomes:

$$(\mathbf{1} - \mathbf{L}) \delta \mathbf{f}^c (\mathbf{1} - \mathbf{R}) = 0 \quad (12.35)$$

where \mathbf{L} and \mathbf{R} are two $D_f \times D_f$ matrices that, since the original basis set $\{\phi_{\mu}(\mathbf{r})\}$ is not orthogonal, are given by:

$$\mathbf{R} = (\mathbf{S}\mathbf{P})\mathbf{P}^T, \quad (12.36)$$

$$\mathbf{L} = (\mathbf{R})^T = \mathbf{P}(\mathbf{S}\mathbf{P})^T; \quad (12.37)$$

here, the $D_f \times n$ matrix \mathbf{P} is defined in Eq. (12.20) and the $D_f \times D_f$ matrix \mathbf{S} is the overlap matrix defining the basis, see Eq. (12.4). In practice, since the dimension

n is usually much smaller than D_f , it is convenient to work with only two matrices \mathbf{P} and \mathbf{SP} ; indeed, all linear operations with \mathbf{L} and \mathbf{R} become much faster when performed in terms of the rectangular matrices \mathbf{P} and \mathbf{SP} .

At this point, we are able to implement the constraint in a simple way. Suppose that we make an unconstrained variation of the pairing function $\delta\mathbf{f}$, then, from this change, we can remove all the contributions that will affect the rank of the matrix (at linear order in the variation) by considering:

$$\delta\mathbf{f}^c = \delta\mathbf{f} - (\mathbf{1} - \mathbf{L})\delta\mathbf{f}(\mathbf{1} - \mathbf{R}). \quad (12.38)$$

This equation represents a linear mapping between unconstrained and constrained variations. It is important to emphasize that this mapping can be considered a simple parametrization of a variation of the geminal function that is constrained to a given number n of molecular orbitals. Moreover, even if \mathbf{f} is restricted to a finite range by introducing R_{cut} , the application of Eq. (12.38) may induce a long-range tail in the geminal function. This approach is useful to represent gapless phases, like metals and nodal superconductors and highlights the reason why the convergence with R_{cut} can be very fast, even in case of metallic behavior.

When applying the optimization techniques described in Chapter 6, we have to compute wave function derivatives with respect to arbitrary variations of the geminal matrix \mathbf{f} . Let us denote the unconstrained derivatives by:

$$D_{\mu,v} = \frac{\partial \ln |F(\mathbf{x})|}{\partial f_{\mu,v}}. \quad (12.39)$$

The total change with respect to the constrained parameters is given by $\text{Tr}[\mathbf{D}(\delta\mathbf{f}^c)^T]$, where $\delta\mathbf{f}^c$ is given by Eq. (12.38). Therefore, we can define the constrained derivatives, i.e., the variations with respect to the parameters that are subject to the constraint:

$$D_{\mu,v}^c = [\mathbf{D} - (\mathbf{1} - \mathbf{L}^T)\mathbf{D}(\mathbf{1} - \mathbf{R}^T)]_{\mu,v}, \quad (12.40)$$

which can be obtained by standard and efficient linear algebra operations.

In summary, the scheme for a constrained optimization of the pairing function is given by:

1. Compute the derivative matrix \mathbf{D} of Eq. (12.39), without taking into account any constraint.
2. Apply the projection of Eq. (12.40) with the current molecular orbitals. By exploiting the fact that all matrices involved are written in terms of small rectangular matrices, a very convenient computation, scaling with $O(n D_f^2)$ can be achieved.

3. After having accumulated enough statistics, apply the steepest-descent method (or more sophisticated schemes, as described in Chapter 6) to obtain $\delta f_{\mu,v} \propto D_{\mu,v}^c$.
4. Obtain the constrained $\delta \mathbf{f}^c$ by using Eq. (12.38).
5. Change the parameters according to:

$$f_{\mu,v} \rightarrow f_{\mu,v} + \delta f_{\mu,v}^c, \quad (12.41)$$

by considering only the ones allowed by the cutoff R_{cut} .

6. Finally, diagonalize \mathbf{f} and keep only the n eigenvectors corresponding to the eigenvalues with the largest absolute values. The new molecular orbitals are then defined after this diagonalization and the corresponding projection matrices \mathbf{L} and \mathbf{R} are re-computed (together with a possible re-computation of the overlap matrix \mathbf{S} whenever also the parameters of the contracted orbitals are also optimized).
7. Repeat all the previous steps until convergence is achieved.

The above algorithm is very stable and general, since it works also when the quasi-particle energies are degenerate at the Fermi energy, which is typical for metallic behavior. Indeed, within this approach the eigenvalues have nothing to do with quasi-particle energies and represent just average occupations of molecular orbitals. In Table 12.1, we report the case of 128 Hydrogens (i.e., 128 electrons) in a body-centered cubic crystal at $r_s = 1.32$.

To achieve a stable convergence to the minimum, it is important that, at each step, when we define the new matrix \mathbf{f} , the non-zero eigenvalues considered are substantially different from zero because if they are too close to zero there may be some problem to set the rank of the matrix within numerical precision. In particular, when $n = N_e/2$ we can, at each iteration of the optimization, reset the largest n eigenvalues $\lambda_\alpha = 1$ (since, as we have discussed, for the Slater determinant the eigenvalues λ_α define only an irrelevant normalization constant) and continue with a very stable optimization.

12.4.1 Beryllium and Fluorine Molecules

Here, we show two examples of the optimization scheme that has been described in the previous section for the F_2 and Be_2 molecules (Marchi et al., 2009). Let us start with the former case, which is relatively simple to treat. Here, the determinant is constructed from a $5s5p2d$ basis of Gaussian orbitals on each ion (leading to $D_f = 60$). The Hartree-Fock approach (with $n = 9$ molecular orbitals), supplemented by the Jastrow factor, gives a considerable error in the binding energy ($E_{\text{binding}} \approx 39mH$, to be compared with the estimated exact value of about $62mH$), while the equilibrium distance is well approximated ($R_{\text{eq}} \approx 2.67a.u.$, which is

Table 12.1. *Optimized energy (a.u.) for 128 Hydrogens in a body-centered cubic crystal at $r_s = 1.32$ as a function of R_{cut} . Twisted boundary conditions with $\theta_x = \theta_y = 2\pi/6$ and $\theta_z = \pi$, see Eq. (12.17) are used. The atomic basis is obtained by contracting the two hybrid orbitals of Eq. (12.15) expanded in a $3s1p$ basis, containing three s -wave (with different exponents $\zeta_{k,l}$) and one p -wave Gaussian orbitals. In order to appreciate the remarkable accuracy obtained with small R_{cut} , we also report the correlated energy difference (computed with the reweighting technique) with respect to the case with $R_{\text{cut}} = 0$. The case with a Slater determinant, taken from a density-functional theory (DFT) calculation, in presence of an optimized Jastrow factor (with two s -wave Gaussian orbitals per atom) is also reported. Notice that already the case with $R_{\text{cut}} = 0$ gives an improvement of about 90% with respect to the latter state.*

R_{cut}	# parameters AGP	Total Energy	Corr. diff.
DFT	0	−64.945(2)	0.064(2)
0	11	−65.009(1)	0.0
2.5	43	−65.010(2)	−0.0018(1)
3	67	−65.017(2)	−0.0064(1)
4	115	−65.014(1)	−0.0072(2)
5	243	−65.015(1)	−0.0072(2)
∞	519	−65.015(2)	−0.0071(2)

compatible with the estimated exact value), see Fig. 12.1. The overall energy dispersion as a function of the relative distance R between the two Fluorine atoms shows up an unphysical maximum at $R \approx 4.5a.u.$ Moreover, at large distances, this wave function, which describes a total singlet, cannot recover the size-consistent result of two Fluorine atoms with $S = 1/2$.

A considerable improvement is achieved by increasing the number of molecular orbitals n . Indeed, already with $n = 10$ the AGP wave function in presence of the Jastrow factor gives a very accurate result for both the binding energy and the equilibrium distance (i.e., $E_{\text{binding}} \approx 61mH$), see Fig. 12.1. Moreover, also size consistency is recovered in this case. By further increasing the number of molecular orbitals, we do not substantially improve the results of $n = 10$. We stress the fact that, by using a single determinant, it is possible to reach an accuracy that is comparable to (if not even better than) the one obtained with quantum-chemistry methods using several thousand determinants.

An interesting example for a diatomic molecule, which represents a real challenge for most of the numerical techniques, is given by the Beryllium dimer.

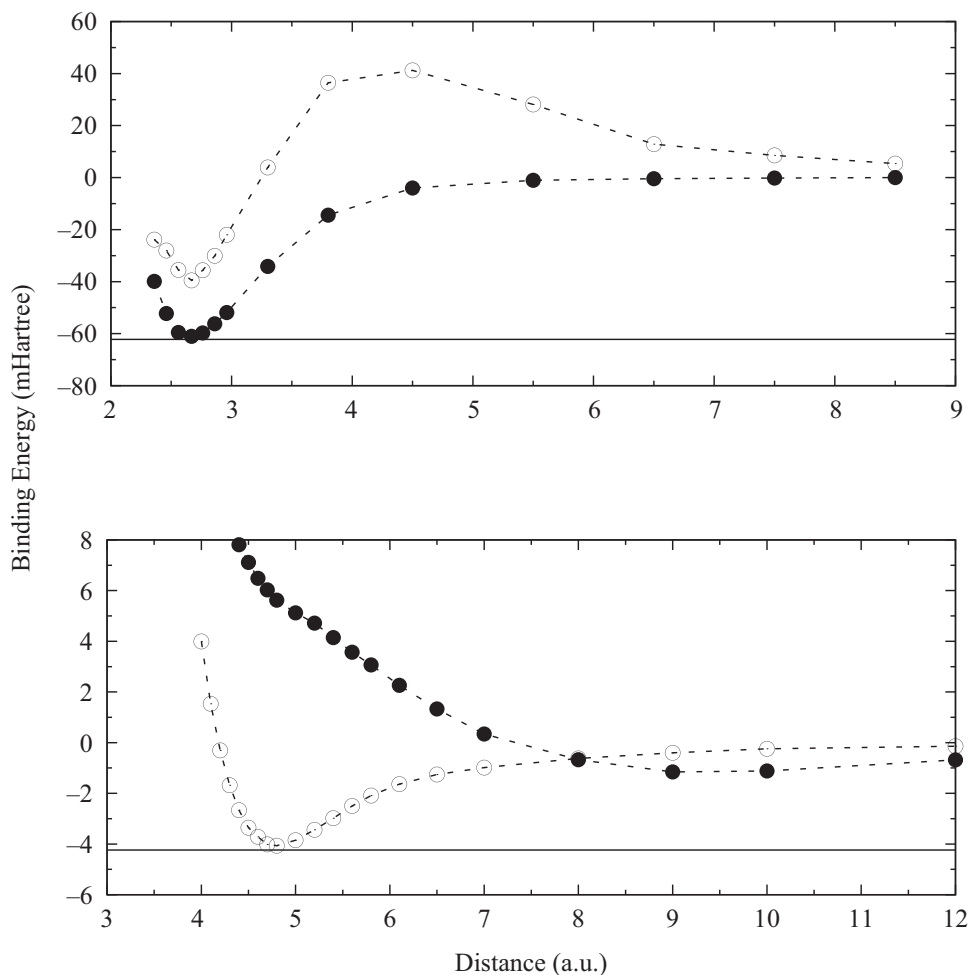


Figure 12.1 Results for the binding energies of the F_2 (upper panel) and Be_2 (lower panel) molecules. The AGP (Hartree-Fock) determinant, supplemented with the Jastrow factor is denoted by filled (empty) circles. The estimated exact results are shown by solid lines. The Hartree-Fock state for the F_2 (Be_2) molecule has $n = 9$ ($n = 4$) molecular orbitals which are constructed from a $5s5p2d$ basis set of Gaussian orbitals ($5s2p1d$ basis set of both Gaussian and Slater types) on each ion. The AGP state for the F_2 (Be_2) molecule has $n = 10$ ($n = 32$) with the same atomic orbitals as the Hartree-Fock wave function. The parameters $\zeta_{k,l}$ are optimized to improve the accuracy of the finite basis set.

Here, the difficulty comes from the small binding energy, for which also the weak Van der Waals forces play an important role. Indeed, the simple Hartree-Fock approach is not able to bind the molecule, while other self-consistent approaches, based upon density-functional theory, widely overestimate the binding energy. We consider a determinant with a $5s2p1d$ basis of both Gaussian and Slater

types on each ion (leading to $D_f = 32$). Remarkably, by considering $n = 4$ molecular orbitals (i.e., the case in which the AGP function corresponds to the Hartree-Fock state), we are able to get excellent results for both the binding energy (e.g., $E_{\text{binding}} \approx 4.1mH$, to be compared with the estimated exact value of about $4.2mH$) and the equilibrium position ($R_{\text{eq}} \approx 4.75a.u.$), see Fig. 12.1. However, by including a larger number of molecular orbitals, the accuracy on the total energy improves, and the overall energy dispersion worsen, giving a much larger bond length and a much smaller binding energy. This outcome is due to the fact that, in this case, the correlated AGP state is much more effective for the single atom (where it reaches 99.9% of the correlation energy) than for the description of the chemical bond.

12.5 Lattice-Regularized Diffusion Monte Carlo

In this section, we will consider an electronic Hamiltonian (written in atomic units) of the form:

$$\mathcal{H} = -\frac{1}{2}\nabla^2 + V(\mathbf{x}) + V_{\text{ii}}, \quad (12.42)$$

where $\nabla^2 = \sum_{i=1}^{N_e} \nabla_i^2$ is the Laplacian operator that defines the total kinetic energy, ∇_i^2 being the corresponding Laplacian operator acting on the single electron with coordinates \mathbf{r}_i , and $V(\mathbf{x}) = V_{\text{ee}}(\mathbf{x}) + V_{\text{ei}}(\mathbf{x})$ is the standard many-body potential, which includes the electron-electron interaction:

$$V_{\text{ee}}(\mathbf{x}) = \sum_{i < j} \frac{1}{|\mathbf{r}_i - \mathbf{r}_j|}, \quad (12.43)$$

and the electron-ion interaction:

$$V_{\text{ei}}(\mathbf{x}) = -\sum_i v_{\text{ei}}(\mathbf{r}_i), \quad (12.44)$$

where

$$v_{\text{ei}}(\mathbf{r}_i) = \sum_I \frac{Z_I}{|\mathbf{r}_i - \mathbf{R}_I|} \quad (12.45)$$

represents its contribution for the electron at position \mathbf{r}_i ; finally, the ion-ion term V_{ii} , which does not depend upon the electron coordinates, is given by:

$$V_{\text{ii}} = \sum_{I < J} \frac{Z_I Z_J}{|\mathbf{R}_I - \mathbf{R}_J|}; \quad (12.46)$$

here, the ion coordinates \mathbf{R}_I with $I = 1, \dots, N_{\text{ion}}$ are just given parameters within the Born-Oppenheimer approximation and, therefore, V_{ii} represents a constant shift of the electronic energy.

In continuous models, the energy spectrum of \mathcal{H} has arbitrary large and positive eigenvalues (e.g., plane waves with large momenta); therefore, in order to filter out the ground-state $|\Upsilon_0\rangle$ from a given trial function $|\Psi_0\rangle$, it is not possible to apply the power method of section 1.7 and it is convenient to introduce an exponential operator:

$$\lim_{\tau \rightarrow \infty} e^{-\mathcal{H}\tau} |\Psi_0\rangle \propto |\Upsilon_0\rangle. \quad (12.47)$$

However, this projector operator is difficult to evaluate exactly for large values of τ . The conventional method is to work in the limit of short time $\Delta\tau$, where the Trotter decomposition gives a small error that vanishes for $\Delta\tau \rightarrow 0$ (Trotter, 1959; Suzuki, 1976a,b), and apply the approximate form several times. Within this approach, there are several approximations that are often not rigorously justified, especially for fermions. Indeed, few aspects of the diffusion Monte Carlo method and the related fixed-node approximation (Kalos et al., 1974; Ceperley and Alder, 1980; Foulkes et al., 2001) are still debated (as for example, how the error vanishes for $\Delta\tau \rightarrow 0$ or the possibility to rigorously define a variational upper-bound property when the so-called pseudo-potentials are used to remove the core electrons).

Here, we take an alternative point of view that relies on a lattice regularization. We start from the approximation of the Laplacian ∇^2 (which defines the kinetic energy of each electron) by using a finite mesh with lattice spacing a :

$$\begin{aligned} \nabla_a^2 g(x, y, z) = & \frac{1}{a^2} [g(x+a, y, z) + g(x-a, y, z) - 2g(x, y, z)] \\ & + \frac{1}{a^2} [g(x, y+a, z) + g(x, y-a, z) - 2g(x, y, z)] \\ & + \frac{1}{a^2} [g(x, y, z+a) + g(x, y, z-a) - 2g(x, y, z)], \end{aligned} \quad (12.48)$$

where $g(x, y, z)$ is a generic function defined in the three-dimensional space (x, y, z) . For $a \rightarrow 0$, the linear operator ∇_a^2 converges to the exact Laplacian with an error that scales as a^2 for a sufficiently regular function g . This fact can be easily found by performing a Taylor expansion of the function $g(x \pm a, y, z)$ (and analogously for the y and z components) and noticing that all the odd derivatives vanish, leaving a residual term that is $O(a^2)$.

In the following, we can define $\nabla_{i,a}^2$ as the Laplacian acting on the single electron coordinate \mathbf{r}_i , according to Eq. (12.48). A lattice regularization of the Hamiltonian \mathcal{H} corresponds to defining an Hermitian operator \mathcal{H}_a , such that $\mathcal{H}_a \rightarrow \mathcal{H}$ for $a \rightarrow 0$; then, the properties of \mathcal{H}_a can be computed numerically with stable simulations,

recovering the ones of the continuous limit for $a \rightarrow 0$. The above requirement is not at all obvious; indeed, the presence of $V_{ei}(\mathbf{x})$, which is an infinitely attractive potential, may lead to the presence of unbounded negative energies. This fact leads us to define a regularization for the electron-ion interaction, whenever the electronic coordinates are too close to the positions of the ions:

$$v_{ei}^a(\mathbf{r}_i) = \sum_I \frac{Z_I}{\text{Max}(|\mathbf{r}_i - \mathbf{R}_I|, a)}, \quad (12.49)$$

which is clearly cutting the Coulomb singularity at small distances. Therefore, the electron-ion potential is modified as:

$$V_{ei}^a(\mathbf{x}) = - \sum_i v_{ei}^a(\mathbf{r}_i). \quad (12.50)$$

It is easy to verify that the regularization of Eq. (12.49) introduces errors in the energy of the same order as those due to the discretization of the Laplacian, as the region where the approximation holds (i.e., $|\mathbf{r} - \mathbf{R}_I| < a$) has a volume that is proportional to a^3 and, in this region, the difference between the original electron-ion potential and the regularized one is on average $O(1/a)$. We also notice that the positive divergence in the electron-electron term $V_{ee}(\mathbf{x})$ does not require a particular attention since an infinite repulsive potential does not affect the existence of a finite ground-state energy.

A natural definition for the lattice regularization would correspond to a simple cubic lattice $\mathbf{r}_{l,m,n} = (la, ma, na)$, where l , m , and n are arbitrary integers. However, this scheme will produce uncontrollable errors as a function of a , since, for not too simple systems, the minimum distance between ion positions and lattice points behaves erratically. In order to improve the convergence for $a \rightarrow 0$ and define an efficient computational scheme, we notice that the operator ∇_a^2 is not necessarily defined on a *regular* lattice. For example, let us consider electrons in a periodic super-cell $L \times L \times L$. Then, whenever the lattice spacing a is not commensurate with the box side L (i.e., L/a is an irrational number, or very close to it, as in any computer implementations) ∇_a^2 will produce electron “hoppings” that will ergodically fill the whole continuous space of the periodic super-cell. In general, also with open systems, it is possible to produce the same effect. By using two incommensurate lattice spacings in the definition of the Laplacian, e.g., $\nabla_a^2 \rightarrow p\nabla_a^2 + (1-p)\nabla_{a'}^2$ with $0 < p < 1$ and a'/a fixed to an irrational number, it is possible to define \mathcal{H}_a acting in the same continuous space of the original Hamiltonian, with the remarkable advantage to improve the smoothness of the extrapolation for $a \rightarrow 0$ (Casula et al., 2005). In the following, we continue to denote this approach as “lattice regularization,” even if the Hamiltonian \mathcal{H}_a acts in the continuum. This is because we have taken the most important advantages of the

lattice: the possibility to enumerate off-diagonal matrix elements of \mathcal{H}_a (see below) and the introduction of a natural cutoff, which is given by the lattice spacing a .

In summary, the lattice regularization of the original Hamiltonian gives:

$$\mathcal{H}_a = -\frac{1}{2}\nabla_a^2 + V^a(\mathbf{x}) + V_{ii}, \quad (12.51)$$

where the potential term is given by:

$$V^a(\mathbf{x}) = V_{ee}(\mathbf{x}) + V_{ei}^a(\mathbf{x}). \quad (12.52)$$

We stress that $\mathcal{H}_a = \mathcal{H} + O(a^2)$ and the fact that both \mathcal{H} and \mathcal{H}_a act on the *same* Hilbert space, as we have explained before. The most important advantage of this approach is that we can apply to the regularized Hamiltonian \mathcal{H}_a the same techniques that we have discussed for lattice models. Indeed, all these techniques are based on the fact that, by applying the Hamiltonian \mathcal{H}_a to one given configuration $|x\rangle$, we obtain a finite number ($6N_e + 1$) of new configurations:

$$\mathcal{H}_a|x\rangle = \left[V^a(\mathbf{x}) + \frac{3N_e}{a^2} \right] |x\rangle - \frac{1}{2a^2} \sum_{j=1}^{6N_e} |x_j\rangle, \quad (12.53)$$

where the second term in the r.h.s. comes from the fact that, according to Eq. (12.48), we have to change every electronic position by $\pm a$, for each cartesian component; in this case, each individual change will produce a new configuration $|x_j\rangle$.

Then, the fixed-node approximation can be applied to \mathcal{H}_a , similarly to the lattice case, see Chapter 10. Here, the fixed-node Hamiltonian $\mathcal{H}_a^{\text{FN},\gamma}$ can be defined in terms of a guiding function $\Psi_G(\mathbf{x})$ that is used to fix the nodal surface of the ground state, see Eq. (10.34). Within this approximation, the off-diagonal matrix elements \mathcal{H}_a that give sign problem are multiplied by $-\gamma$, where γ is an arbitrary positive number, while the diagonal elements are changed according to:

$$V^a(\mathbf{x}) \rightarrow V^a(\mathbf{x}) + (1 + \gamma)V_{\text{sf}}^a(\mathbf{x}), \quad (12.54)$$

with

$$V_{\text{sf}}^a(\mathbf{x}) = -\frac{1}{2a^2} \sum_{j:s(\mathbf{x},\mathbf{x}_j)<0} \frac{\Psi_G(\mathbf{x}_j)}{\Psi_G(\mathbf{x})}, \quad (12.55)$$

where $s(\mathbf{x}, \mathbf{x}_j) = \Psi_G(\mathbf{x}_j)\Psi_G(\mathbf{x})$. It is interesting to discuss the consequences of this approach for $a \rightarrow 0$. Since the condition $\Psi_G(\mathbf{x}_j)\Psi_G(\mathbf{x}) < 0$ is verified only very close (i.e., at distance $\approx a$) to the nodal surface where $\Psi_G(\mathbf{x}) = 0$, the matrix elements of $\mathcal{H}_a^{\text{FN},\gamma}$ will almost always coincide with the matrix elements of \mathcal{H}_a . For the same reason, the potential $V_{\text{sf}}^a(\mathbf{x})$ is non-zero only close to the nodal surface. Therefore, we obtain that for $a \rightarrow 0$, the fixed-node Hamiltonian will differ from

the regularized one by a boundary condition at the nodal surface, where the fixed-node ground state of $\mathcal{H}_a^{\text{FN},\gamma}$ vanishes. Indeed, the potential $V_{\text{sf}}^a(\mathbf{x})$ diverges for $a \rightarrow 0$ and wave functions that do not vanish in the nodal surface will have an infinite (positive) expectation value of $\mathcal{H}_a^{\text{FN},\gamma}$ for $a \rightarrow 0$. Therefore, in this limit we clearly see that the fixed-node approximation with the lattice regularization is equivalent to a boundary condition and provides the best variational energy compatible with the nodes of the guiding function. Notice that this fact is obtained without using the so-called tilling theorem (Ceperley, 1991), since the fixed-node Monte Carlo sampling on the lattice is always ergodic for $\gamma > 0$ and $a > 0$ and the ground state of $\mathcal{H}_a^{\text{FN},\gamma}$ is defined in all nodal pockets. In particular, the simulation with $\gamma = 1$ is the most efficient one, while the case with $\gamma = 0$ is not ergodic because the nodal pockets cannot be crossed.

Then, the fixed-node approach can be implemented within the Green's function Monte Carlo algorithm; however, since the spectrum of the Hamiltonian is not bounded from above, it is necessary to consider the continuous-time limit, which has been described in section 8.4. In this way, we obtain the approximate ground state, which fulfills the fixed-node constraint given by the guiding function $\Psi_G(\mathbf{x})$, in analogy to the standard diffusion Monte Carlo framework (Casula et al., 2005). We remark that the conventional diffusion Monte Carlo technique has a time-step error in $\Delta\tau$, while the present formulation yields a lattice-space error; both approaches share the same upper-bound property and converge to the same projected fixed-node energy, in the limit $\Delta\tau \rightarrow 0$ and $a \rightarrow 0$, respectively.

12.6 An Improved Scheme for the Lattice Regularization

Unfortunately, although it is possible to obtain a remarkably smooth convergence with $a \rightarrow 0$, this simple approach is not very useful in practice, as the error is often large, implying that an exceedingly small value of a is necessary to obtain accurate results. In order to improve the convergence for $a \rightarrow 0$, we should consider an alternative approach, in which the Laplacian is still discretized by using Eq. (12.48) and a different version of the potential operator is considered, i.e., $V(\mathbf{x}) \rightarrow V_{\text{zv}}^a(\mathbf{x})$. In practice, inspired from the fixed-node approximation on a lattice, we can modify the potential operator by requiring that the local energy of the original Hamiltonian coincides with that of the regularized one:

$$\frac{\langle x | \mathcal{H}_a | \Psi_G \rangle}{\langle x | \Psi_G \rangle} = \frac{\langle x | \mathcal{H} | \Psi_G \rangle}{\langle x | \Psi_G \rangle}. \quad (12.56)$$

This equality is assumed to be fulfilled for the best guiding function $|\Psi_G\rangle$ (i.e., the one corresponding to the lowest variational energy). This is a useful condition because it satisfies the zero-variance property, also in the presence of the lattice

regularization: if the guiding function coincides with an exact eigenstate, then the local energy of \mathcal{H}_a is equal to the exact eigenvalue and the corresponding fixed-node energy will be exact, regardless on the magnitude of a . Then, Eq. (12.56) implies a unique definition of $V_{zv}^a(\mathbf{x})$. Indeed, if we assume that the Laplacian is discretized by the replacement $\nabla^2 \rightarrow \nabla_a^2$, then $V_{zv}^a(\mathbf{x})$ is given by:

$$V_{zv}^a(\mathbf{x}) = V(\mathbf{x}) + \frac{(\nabla_a^2 - \nabla^2) \Psi_G(\mathbf{x})}{2\Psi_G(\mathbf{x})}, \quad (12.57)$$

which gives that $V_{zv}^a(\mathbf{x}) \rightarrow V(\mathbf{x})$ for $a \rightarrow 0$. This choice has been originally proposed by Casula et al. (2005). There, the simulations were very stable and the limit $a \rightarrow 0$ was extracted in an easy way; unfortunately, the calculations are not generally well defined for fermions, as the Hamiltonian \mathcal{H}_a does not always have a finite ground-state energy for $a > 0$. Indeed, the regularized potential $V_{zv}^a(\mathbf{x})$ can assume, close to the nodal surface of the guiding function $\Psi_G(\mathbf{x})$, unbounded negative values, which cannot be compensated by the lattice-regularized kinetic energy (whose matrix elements are always finite). Nevertheless, a simulation with a limited amount of computer resources may produce reasonable results, since it is very difficult, with a statistical method, to select the configurations on the nodal surface causing the instability. However, the possibility of having instabilities cannot be excluded *a priori* and it is important to find a solution to this possible catastrophe. A similar scenario is often reported also in the standard diffusion Monte Carlo technique (Foulkes et al., 2001; Umrigar et al., 1993), especially when pseudo-potentials are used. In the latter case, for a given $\Delta\tau$, a general remedy to this catastrophe does not exist yet, although it is widely believed that, for small enough $\Delta\tau$ simulations should be stable with appropriate cutoffs. Within the lattice-regularized approach, the situation is more transparent and a simple remedy can be found, as we will describe in the following.

In order to define a rigorously stable and robust method that works for *any* finite value of a , we need to modify the electron-ion interaction. In particular, we notice that the regularization of Eq. (12.57) just corresponds to the modification of the electron-ion potential by replacing in Eq. (12.45):

$$v_{ei}(\mathbf{r}_i) \rightarrow v_{zv,i}^a(\mathbf{x}), \quad (12.58)$$

where

$$v_{zv,i}^a(\mathbf{x}) = v_{ei}(\mathbf{r}_i) + \frac{(\nabla_{i,a}^2 - \nabla_i^2) \Psi_G(\mathbf{x})}{2\Psi_G(\mathbf{x})}. \quad (12.59)$$

Then, with a good guiding function, which satisfies the electron-ion cusp conditions (as discussed in section 12.2), the above replacement cancels out most of the singularities of the attractive potential; however, we can still have unbounded negative

values on the nodal surface of the guiding function $\Psi_G(\mathbf{x})$. A safe possibility to protect the simulation from *all* possible instabilities coming from the nodal surface of the guiding function is given by the following modification of the electron-ion potential for each electron i :

$$v_{\max,i}^a(\mathbf{x}) = \text{Max} [v_{zv,i}^a(\mathbf{x}), v_{\text{ei}}^a(\mathbf{r}_i)], \quad (12.60)$$

where $v_{\text{ei}}^a(\mathbf{r}_i)$ is defined in Eq. (12.49). Within this formulation, the regularized potential is protected from the possible instabilities close to the nodal surface and guarantees the existence of a finite ground-state energy for any $a > 0$. Since the condition $v_{\text{ei}}^a(\mathbf{r}_i) > v_{zv,i}^a(\mathbf{x})$ is often satisfied, this choice can be improved by applying the condition (12.60) only when electrons are very close to the nodal surface. For this purpose, we apply the (single-electron) condition (12.60) only when the electrons cross the nodal surface with the discretized Laplacian:

$$v_{\text{opt},i}^a(\mathbf{x}) = \begin{cases} v_{\max,i}^a(\mathbf{x}) & \text{if } \Psi_G(\mathbf{x})\Psi_G(\mathbf{x}_j) < 0 \text{ for at least one } \mathbf{x}_j, \\ v_{zv,i}^a(\mathbf{x}) & \text{otherwise;} \end{cases} \quad (12.61)$$

here, \mathbf{x}_j indicates the possible configurations, generated by the discretized Laplacian $\nabla_{a,i}^2$ for the electron i . Notice that, for finite values of the lattice spacing a , the above condition could miss the cases where a double sign change occurs. However, this circumstance has a negligible effect for small values of a . In Fig. 12.2, we report the results of the previously defined schemes for the case of 18 equally spaced Hydrogens placed in a one-dimensional chain (where nearest-neighbor atoms are at distance $R = 2a.u.$). Here, the guiding function is given by an optimized Jastrow factor (with a $3s2p1d$ basis) applied to a Slater determinant that is obtained from a density-functional calculation with a $4s2p1d$ basis. The most simple approach, defined by Eq. (12.57) with no further regularization, already gives quite accurate results. By imposing the modification of Eq. (12.60), we obtain much higher energies, suggesting that this kind of scheme is too strict. Finally, very accurate and smooth energies are obtained within the final choice of Eq. (12.61), indicating that this approach gives the best possible approximation for the lattice-regularized diffusion Monte Carlo method.

This scheme for the lattice regularization is perfectly size consistent, whenever the guiding function is also size consistent. In fact, let us consider a wave function $\Psi_G(\mathbf{x})$ that factorizes at large distances:

$$\Psi_G(\mathbf{x}) \approx \Psi_G^A(\mathbf{x}_A)\Psi_G^B(\mathbf{x}_B), \quad (12.62)$$

where we assume that the relevant electronic configurations \mathbf{x} are obtained by N_A (N_B) electrons corresponding to a configuration \mathbf{x}_A (\mathbf{x}_B) within the region A (B).

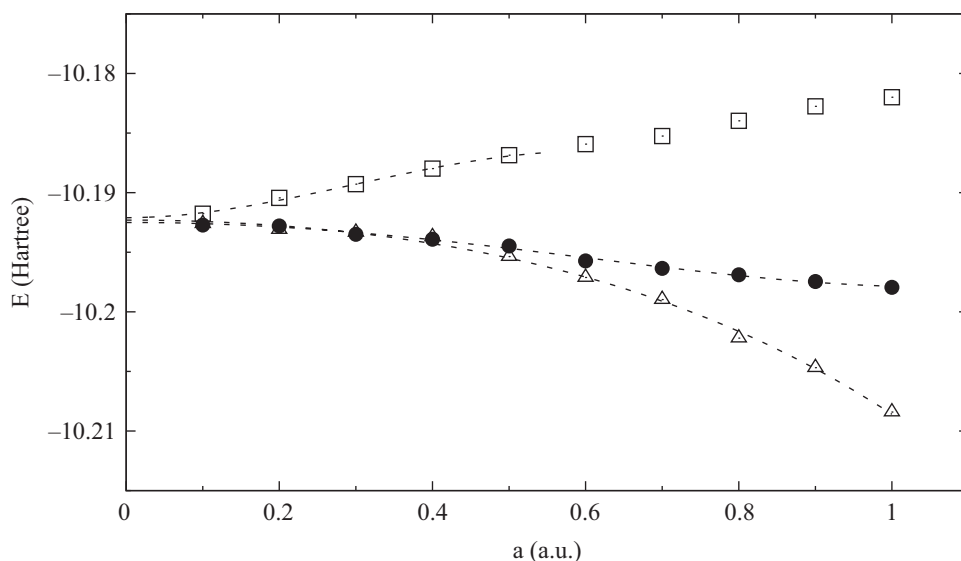


Figure 12.2 Results for different regularization schemes for the total energy of 18 Hydrogens (i.e., 18 electrons) placed in a one-dimensional chain at distance $R = 2a.u.$. The guiding function used here is obtained by applying an optimized Jastrow factor (with a $3s2p1d$ basis) on a Slater determinant obtained by a density-functional calculation with a $4s2p1d$ basis. The simple approximation of Eq. (12.57) (empty triangles), the one given by Eq. (12.60) (empty squares), and the one given by Eq. (12.61) (full circles) are reported. The $a \rightarrow 0$ extrapolated energy is $E = -10.1925(2)$ Hartree.

Then, the regularized potential of Eq. (12.59) will act independently in the two regions:

$$v_{zv,i}^a(\mathbf{x}) = \begin{cases} v_{ei}(\mathbf{r}_i) + \frac{(\nabla_{i,a}^2 - \nabla_i^2) \Psi_G^A(\mathbf{x}_A)}{2\Psi_G^A(\mathbf{x}_A)} & \text{if } \mathbf{r}_i \in A, \\ v_{ei}(\mathbf{r}_i) + \frac{(\nabla_{i,a}^2 - \nabla_i^2) \Psi_G^B(\mathbf{x}_B)}{2\Psi_G^B(\mathbf{x}_B)} & \text{if } \mathbf{r}_i \in B, \end{cases} \quad (12.63)$$

which lead to:

$$v_{\max,i}^a(\mathbf{x}) = v_{\max,A,i}^a(\mathbf{x}_A) + v_{\max,B,i}^a(\mathbf{x}_B). \quad (12.64)$$

This fact explains the reason why we have done a regularization that considers each single-electron contribution independently, see Eq. (12.60). By contrast, a regularization that takes $V_{\max}^a(\mathbf{x}) = \text{Max}[V_{zv}^a(\mathbf{x}), V^a(\mathbf{x})]$, where $V^a(\mathbf{x})$ is given by Eq. (12.50), is not size consistent, as the global relation implied by the Max operation unavoidably couples the two regions A and B , even when they are at large distance.

Finally, the lattice-regularized approach can be naturally extended to the use of pseudo-potentials, which are usually considered to remove the large energy scales coming from the core electrons. The pseudo-potentials have terms that simply add to $v_{ei}(\mathbf{r}_i)$ with a non-local contribution, which has a natural description by means of lattice operators. Indeed, they can be safely considered as further hopping terms to be included in the regularized Laplacian ∇_a^2 . Therefore, it is straightforward to apply the fixed-node scheme described before, maintaining its upper bound property for the energy. Moreover, the use of soft pseudo-potentials (that cancel the electron-ion singularity) leads to a smooth local potential that does not need to be regularized, so that the regularization of Eq. (12.49) does not have to be applied.